# Subwavelength engineering for Brillouin gain optimization in silicon optomechanical waveguides

**Jianhao Zhang,[1] Omar Ortiz,[1] Xavier Le-Roux,[1] Eric Cassan,[1] Laurent Vivien,[1] Delphine Marris-Morini,[1] Daniel Lanzillotti Kimura,[1] Carlos Alonso-Ramos[1]**

[1] Centre de Nanosciences et de Nanotechnologies, Université Paris-Saclay, Univ. Paris-Sud, CNRS, 91120, Palaiseau, France.

*e-mail: jianhao.zhang@c2n.upsaclay.fr*

## ABSTRACT

Brillouin optomechanics has recently emerged as a promising tool to implement new functionalities in silicon photonics, including high-performance opto-RF processing and non-reciprocal light propagation. One key challenge in this field is to maximize the photon-phonon interaction and the acoustic lifetime, simultaneously. Here, we propose a new strategy that exploits subwavelength engineering of the photonic and phononic modes in silicon membrane waveguides to maximize the Brillouin gain. The proposed optomechanical waveguide comprises a lattice of holes with a period in the subwavelength regime for near-infrared photons and GHz phonons. By properly designing the dimensions of the subwavelength periodic structuration, we tightly confine optical and acoustic modes, minimizing leakage losses and maximizing the Brillouin coupling. Our theoretical analysis predicts a high acoustic quality factor of up to 2000 and a remarkable Brillouin gain yielding 10000 $(\mathrm{W}\cdot\mathrm{m})^{-1}$. We believe that the proposed subwavelength-nanostructured waveguide holds a great potential for the engineering of Brillouin optomechanical interactions in silicon.

**Keywords**: Silicon photonics, optomechanics, nonlinear optics, subwavelength structures, Brillouin.

## INTRODUCTION

Brillouin scattering is a third order optical nonlinear process that results from light-sound coupling [1]. This effect has been widely explored in the context of laser physics, microwave-frequency acoustic excitation and precision spectroscopy, among others. The availability of materials co-confining phonons and photons in the same device [2-4] has enabled the demonstration of Brillouin scattering on chip [5-7], showing exceeding strengths over Kerr and Raman interactions. Over the past decade, there have been remarkable achievements in the control of on-chip Brillouin optomechanics using chalcogenide-based materials [5], gallium arsenide [2, 4, 8] and silicon [9]. Acoustic phonons with GHz frequencies in nanometric-scale waveguides have wavelengths close to one micron. Thus, they can strongly interact with in-phase lightwaves in the near-infrared [10-13]. This high-efficiency coupling enabled remarkably large Brillouin gain [14] and even Brillouin laser [15] in silicon. Silicon membranes have been identified as a promising solution to efficiently confine photons and phonons [9, 11, 15]. However, the phonon lifetime in silicon membranes may be limited by acoustic leakage, from the waveguide core to the lateral silicon slabs or silica substrate. This loss has been alleviated by inserting air gaps [14, 15] or by implementing phononic stop bands in the transversal dimension [16]. The former approach may result in reduced photon-phonon overlap because the expanded phonons distribution along the Si slab between the air gaps, limiting the gain to $1000\ (W\cdot m)^{-1}$ [14]. The latter provided higher calculated Brillouin gain of $1750\ (W\cdot m)^{-1}$ [16], but is limited in bandwidth, as only the phonons within the stop-band are confined. Here, we propose a new waveguide geometry that exploits geometrical subwavelength softening to minimize the lateral leakage of the acoustic modes and subwavelength index engineering to confine optical modes. By working well below the photonic and phononic bandgaps, the proposed subwavelength-lattice waveguide allows to simultaneously enhance the photon-phonon interaction and increase the quality factor of the acoustic mode, while overcoming the typical bandwidth limitations of phononic and phoxonic crystals. Our calculations show that the proposed waveguide may provide Brillouin gain as high as $10000\ (W\cdot m)^{-1}$.

## 1. PROPOSED GEOMETRY

As shown in Fig. 1 (a), the proposed membrane waveguide consists of a central strip and a lattice of lateral arms that anchor the waveguide core to the infinite silicon slab. The acoustic confinement in our structure is achieved by giant impedance mismatch between the air and the silicon core, instead of a phononic Bragg mirror, while the arm lattice with subwavelength period introduces a small acoustic dissipation. The strip has a width of $w_{wg} = 500$ nm and a thickness of $t_{wg} = 220$ nm, while the arms have a width of $w_{arms} = 2.5$ μm and a thickness of $t_{arms} = 50$ nm. Silicon waveguides with lateral subwavelength cladding have been used for mid-infrared optical propagation [17], and thermo-optical devices [18]. More recently, Si membranes with periodic arms in the cladding have also been studied for the optimization of Brillouin scattering [16]. However, the period of the arms

was substantially larger than the acoustic wavelength and the lateral acoustic confinement required the implementation of a Bragg corrugation in the transversal dimension. Here, we choose a period of $p = 240$ nm, well below the acoustic wavelength (1.07 μm in silicon, at 9GHz) and optical wavelength (640 nm in silicon, i.e. 1550 nm in vacuum).

As an example, the normalized intensity profile of the subwavelength optical mode, at 195THz, collected from plane I and II is shown in Figs 1 (b) and (c), respectively.

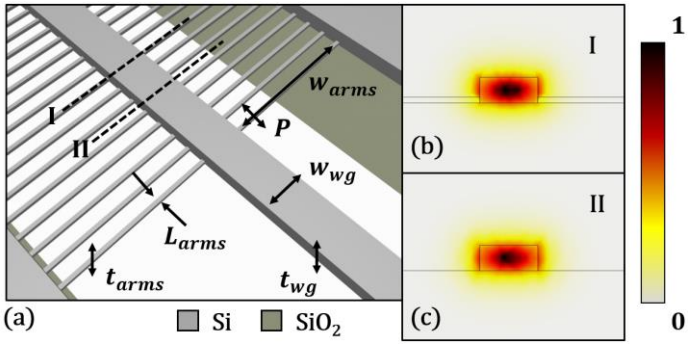


Fig. 1. (a) Schematic of the proposed subwavelength-lattice silicon waveguide. Optimized dimensions: $t_{arms} = 50nm$, $t_{wg} = 220nm$, $w_{wg} = 500nm$ and $p = 240nm$. $w_{arms} = 2.5um$ The Brillouin performance is studied as a function of the length of the arms, $L_{arms}$. Normalized intensity of the electric field collected at (b) plane I and (c) plane II, defined in schematic geometry in (a).

## 2. OVERVIEW OF OPTOMECHANICAL PERFORMANCE

Three cascaded unit cells of the proposed optomechanical waveguide are shown in the inset of Fig. 2, together with the distribution of the transverse acoustic mode (with frequency at 9 GHz), calculated using finite element methods (FEM) model. The maximum displacement occurs for the waveguide core along the arm direction (*x*) indicated by the black arrows. Flexural displacement takes place in the silicon arms. The high acoustic velocity (~9000m/s) results in an acoustic wavelength around 1 μm, which is on the same order as optical wavelength at telecom frequency. Thus, the lattice period of $p = 240$ nm, is well below half of the optical wavelength, suppressing diffraction effects that may arise from the periodicity. Hence, this periodic structure can be described as a subwavelength-lattice waveguide grating for the acoustic mode, doing an analogy with optical subwavelength grating waveguide membranes [17].

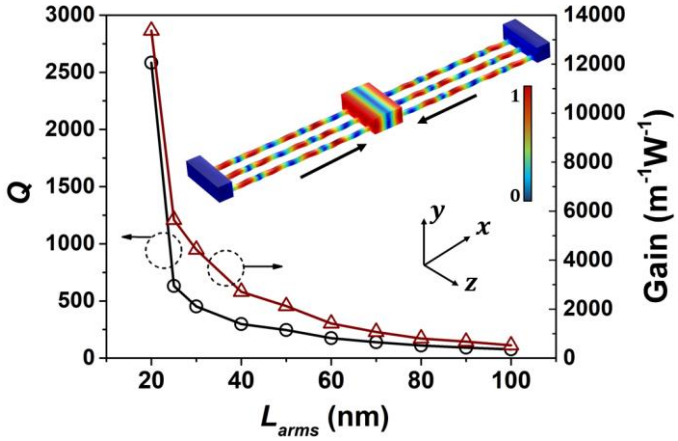


Fig. 2. (a) The quality factor of the acoustic mode and the overall Brillouin gain as a function of the length of silicon arms $L_{arms}$. Inset is the normalized displacement profile of the acoustic mode with a frequency of 9.1 GHz. The strain direction of the silicon core is shown by the thick, black arrows.

We have calculated the quality factor (*Q*) of the acoustic mode using FEM model, considering the loss from surrounding air, loss from the acoustic leakage to the infinite slab and the thermo-elastic loss. As shown in Fig. 2 (black line), *Q* changes nonlinearly with the length of the arms. A remarkable *Q* of up to 1200 can be obtained for an arm length of 25 nm.

The Brillouin gain can be calculated with an integrated optical force [9-13] distributed in the whole unit cell:

$$G = \frac{2\omega_p Q_A}{\tilde{m}_{eff}\Omega_A^2} S(f) \left| \frac{1}{p} \int f_d dv \right|^2. \quad (1)$$

In equation (1), $\omega_p$, $\Omega_A$ and are the angular frequencies of the optical and acoustic modes, respectively, $Q_A$ is the quality factor of the acoustic mode, $\tilde{m}_{eff}$ is the mass density per unit propagation length. $S(f)$ is the Lorentzian-shape spectrum of Brillouin gain and $S(\Omega_A/2\pi)$ indicate the maximum gain. The optical force density $f_d$ includes the optimized overlap between the optical and mechanical modes and is governed mainly by the radiation pressure

force and electrostriction calculated from photo-elastic tensors. The Brillouin gain, calculated as a function of the arm length, $l_{arms}$, is shown in Fig. 2 (red line). The Brillouin gain increases sharply when the arm length is below 30 nm. For an arm length of 20 nm the Brillouin gain can increase up to $10000\ (W \cdot m)^{-1}$. For an arm length of 50 nm, compatible with electron-beam lithography, the Brillouin gain is $2000\ (W \cdot m)^{-1}$. This gain value compares favorably with previously proposed silicon membranes with periodic silicon arms [14], while obviating the need for transversal Bragg phononic mirrors.

## 3. CONCLUSION

We proposed and analyzed a new strategy to optimize Brillouin scattering in silicon membrane waveguides. The proposed waveguide geometry confines mechanical and optical modes by subwavelength softening and subwavelength index engineering, respectively. By working well below the photonic and phononic bandgaps, this proposed subwavelength-lattice waveguide allows to simultaneously enlarge the photon-phonon interaction and increase the quality factor of the acoustic mode, obviating the typical bandwidth limitations of phononic and phoxonic crystals [16]. Our calculations show that the proposed waveguide may provide high acoustic quality factor up to 2000 and Brillouin gain up to 10000 $(W \cdot m)^{-1}$ in the most severe clean room fabrication conditions. These results confirm the possibility to simultaneously shape the propagation of acoustic and optical modes with silicon subwavelength structures. We believe these results will expedite the exploration in photon-phonon interaction based on subwavelength-lattice waveguides.

## 4. ACKNOWLEDGEMENTS

Agence Nationale de la Recherche (MIRSPEC ANR-17-CE09-0041, BRIGHT ANR-18-CE24-0023-01) is acknowledged for supporting this work.

## REFERENCES

[1] G. P. Agrawal, *Nonlinear Fiber Optics*., 5th ed., Rochester, New York, USA, 2013, pp. 1–21.
[2] M. Esmann, *et al.*: Brillouin scattering in hybrid optophononic Bragg micropillar resonators at 300 GHz, *Optica*, vol. 6, pp. 854-859. 2019.
[3] G. Arregui, *et al.*: Anderson photon-phonon colocalization in certain random superlattices, *Phys. Rev. Lett.*, vol. 122, p. 043903, 2019.
[4] F.R. Lamberti, *et al.*: Optomechanical properties of GaAs/AlAs micropillar resonators operating in the 18 GHz range, *Opt. Express*, vol. 25, pp. 24437-2447. 2017.
[5] R Pant, *et al.*: On-chip stimulated Brillouin scattering, *Opt. Exp.*, vo. 19, pp. 8285-8290, 2011.
[6] B. J. Eggleton, *et al.*: Brillouin integrated photonics, *Nat. Photon.*, vo. 13, pp. 664-677, 2019.
[7] A. H. Safavi-Naeini, *et al.*: Controlling phonons and photons at the wavelength scale: integrated photonics meets integrated phononics, *Optica*, vol. 6, pp. 213-231. 2019.
[8] F. Kargar, *et al.*: Direct observation of confined acoustic phonon polarization branches in free-standing semiconductor nanowires, *Nat. Comm.*, vol. 7, p. 13400. 2016.
[9] P. T. Rakich, *et al.*: Giant enhancement of stimulated Brillouin scattering in the subwavelength limit, *Phys. Rev. X*, vo. 2, p. 011008, 2012.
[10] W. Qiu, *et al.*: Stimulated Brillouin scattering in nanoscale silicon step-index waveguides: a general framework of selection rules and calculating SBS gain, *Opt. Exp.*, vo. 21, pp. 31402-31419, 2013.
[11] R. Van Laer, *et al.*: Interaction between light and highly confined hypersound in a silicon photonic nanowire, *Nat. Photon.*, vo. 9, pp. 199-203, 2015.
[12] C. J. Sarabalis, *et al.*: Guided acoustic and optical waves in silicon-on-insulator for Brillouin scattering and optomechanics, *APL Photonics*, vo. 1, p. 071301, 2016.
[13] C. Wolff, *et al.*: Stimulated Brillouin scattering in integrated photonic waveguides: Forces, scattering mechanisms and coupled-mode analysis, *Phys. Rev. A*, vo. 92, p. 013836, 2015.
[14] E. A. Kittlaus, *et al.*: Large Brillouin amplification in silicon, *Nat. Photon.*, vo. 10, pp. 463-468, 2015.
[15] N. T. Otterstrom, *et al.*: A silicon Brillouin laser, *Science*, vo. 360, pp. 1113-1116, 2016.
[16] M. K. Schmid, *et al.*: Suspended mid-infrared waveguides for stimulated Brillouin scattering, *Opt. Exp.*, vo. 27, pp. 4976-4989, 2019.
[17] J. S. Penades, *et al.*: Suspended silicon mid-infrared waveguide devices with subwavelength grating metamaterial cladding, *Opt. Exp.*, vo. 24, pp. 22909-22916, 2018.
[18] J. Zhang, S. He: Cladding-free efficiently tunable nanobeam cavity with nanotentacles, *Opt. Exp.*, vo. 25, pp. 12541-12551, 2017.